



## Enhanced angiogenic effects of RGD, GHK peptides and copper (II) compositions in synthetic cryogel ECM model

Mohamed Zoughaib<sup>a</sup>, Duong Luong<sup>a</sup>, Ruslan Garifullin<sup>a,b</sup>, Dilara Z. Gatina<sup>a</sup>, Svetlana V. Fedosimova<sup>a</sup>, Timur I. Abdullin<sup>a,\*</sup>

*Institute of Fundamental Medicine and Biology, Kazan Federal University, 420008 Kazan, Russia*  
*Institute of Materials Science and Nanotechnology, Bilkent University, 06800 Ankara, Turkey*

### ARTICLE INFO

#### Keywords:

Tissue regeneration  
 Synthetic cryogels  
 RGD  
 GHK  
 Copper  
 Glutathione  
 Cytokines  
 Therapeutic angiogenesis

### ABSTRACT

Synthetic oligopeptides are a promising alternative to natural full-length growth factors and extracellular matrix (ECM) proteins in tissue regeneration and therapeutic angiogenesis applications. In this work, angiogenic properties of dual and triple compositions containing RGD, GHK peptides and copper (II) ions ( $\text{Cu}^{2+}$ ) were for the first time studied. To reveal specific in vitro effects of these compositions in three-dimensional scaffold, adamantyl group bearing peptides, namely Ada-Ahx-GGRGD (1) and Ada-Ahx-GGGHK (2), were effectively immobilized in bioinert pHEMA macroporous cryogel via host-guest  $\beta$ -cyclodextrin-adamantane interaction. The cryogels were additionally functionalized with  $\text{Cu}^{2+}$  via the formation of GHK-Cu complex. Angiogenic responses of HUVECs grown within the cryogel ECM model were analyzed. The results demonstrate that the combination of RGD with GHK and further with  $\text{Cu}^{2+}$  dramatically increases cell proliferation, differentiation, and production of a series of angiogenesis related cytokines and growth factors. Furthermore, the level of glutathione, a key cellular antioxidant and redox regulator, was altered in relation to the angiogenic effects. These results are of particular interest for establishing the role of multiple peptide signals on regeneration related processes and for developing improved tissue engineering materials.

### 1. Introduction

Providing effective angiogenesis is one of the most challenging problems in posttraumatic tissue regeneration using tissue replacement and engineering materials. It requires proper combination and organization of extracellular matrix (ECM) components and signaling molecules to direct functional activity of cells involved in the generation of new microvessels. During recent decades, substantial efforts have been devoted to the development of biomaterials mimicking native microenvironment of endothelial cells (ECs) and promoting angiogenic responses. Polymer hydrogels have been particularly exploited to construct artificial ECMs as these materials respond to hydration and physicochemical properties of soft and newly formed tissues [1].

Several types of ECM-derived hydrogel materials (HMs) mostly based on collagen [2], gelatin [3], hyaluronic acid [4], fibrin [5] and their composites with synthetic polymers [6] have been previously used to study the behavior of ECs and other regeneration-related cells in ECM-mimicking scaffolds. The ability of HMs to guide cell functions and

facilitate angiogenesis can be improved via combination with different growth factors (GFs) supplemented in growth media or, often preferably, introduced to the materials by different ways. For instance, covalently immobilized VEGF and angiopoietin-1 in collagen scaffolds were reported to increase EC density and capillary tube formation [7]. Likewise, VEGF and PDGF loaded into polycaprolactone/collagen/hyaluronic acid hybrid hydrogel enhanced the attachment and infiltration of ECs within the material [6]. The therapeutic use of natural GFs such as recombinant polypeptides, however, has major limitations associated with high cost of purified GFs, retained risk of immunogenicity, low stability and difficulties of controllable immobilization in materials.

Synthetic oligopeptides are capable of reproducing minimal bioactive peptide sequences of full-length GFs and ECM components, and therefore they are a promising alternative to natural proteins upon tissue regeneration. These oligopeptides are versatile biomolecules which can specifically interact with cellular targets associated with cell proliferation, growth and differentiation [8,9]. Established techniques for peptide synthesis and functionalization allow producing safe, stable and

\* Corresponding author.

E-mail address: [timur.abdullin@kpfu.ru](mailto:timur.abdullin@kpfu.ru) (T.I. Abdullin).

<https://doi.org/10.1016/j.msec.2020.111660>

Received 15 July 2020; Received in revised form 24 September 2020; Accepted 18 October 2020

Available online 21 October 2020

0928-4931/© 2020 Elsevier B.V. All rights reserved.

inexpensive oligopeptides which can be readily incorporated into HMs [8]. The oligopeptides are also of particular interest as a simplified model of complex proteinaceous matrix to help studying peptide signals involved in tissue development and degeneration, which are still quite poorly known. Preferably, the oligopeptides should be combined with bioinert scaffolds that, in contrary to naturally-derived materials, provide chemical control over the bioactive component, allowing identification of defined peptide signals under three-dimensional conditions [10–12].

To date, most studies on regenerative effects of oligopeptides in tissue engineering materials concern cell adhesion motifs of ECM proteins such as fibronectin and laminin-derived RGD, IKVAV and YIGSR based sequences [13–17]. Beyond their adhesive ability, these oligopeptides were shown to induce various biological responses. RGD promoted osteogenic differentiation of mesenchymal stem cells [13] and ECM deposition by chondrocytes [15] in alginate and agarose-PEGDA hydrogels, respectively. IKVAV-conjugated polyethylene glycol (PEG) hydrogels supported neuronal differentiation of murine embryonic stem cells [16], whereas YIGSR improved the mobility and guided the migration of ECs on pHEMA material [17]. When presented in combination with RGD in PEG hydrogels, YIGSR peptide enhanced EC migration compared with RGD alone [18]. Similarly, coimmobilization of RGD and IKVAV/YIGSR in PEG diacrylate hydrogel resulted in improved cell adhesion, survival, tubulogenesis and vessel morphology over the individual peptides [10]. In view of these data, searching multiple combinations of oligopeptides as well as other small molecule factors is of current importance to design highly effective materials for tissue engineering and regeneration applications.

Among short peptides, ECM-derived tripeptide GHK found in type I collagen, osteonectin, thrombospondin-1, and fibrin [19] and its naturally occurring copper complex (GHK-Cu) have gained much attention as multifunctional cellular modulators with proved beneficial effects in wound healing, ECM biosynthesis, tissue degeneration and aging [20,21]. Furthermore, copper is an essential microelement, cofactor of critical metabolic enzymes [22], and established angiogenic factor [23]. Copper (II) ions were reported to stimulate migration and tube-forming ability of human ECs [24]. GHK is considered a transport form of  $\text{Cu}^{2+}$ , which provides living cells and tissues with the active metal ions [25], while decreases their side effects in vivo [26]. GHK-Cu was reported to cause increased responses in murine wound repair and hair growth models compared with copper-free GHK [27].

Recently, we demonstrated that RGD and GHK peptides in dual composition exhibit synergistic mitogenic activity toward mammalian cells and dramatically alter their behavior in HMs [28]. To reveal such an activity, we designed a synthetic ECM model consisting of pHEMA/PEG/ $\beta$ -cyclodextrin macroporous cryogels, which was functionalized with adamantylated RGD and GHK peptides in a controllable manner via host-guest interactions. This cryogel based model was proved to be an informative tool to study multiple cell-responsive factors within ECM-mimicking scaffold. In the current work, this model was employed for accurate examination and comparison of angiogenic effects of dual and triple compositions of RGD, GHK and  $\text{Cu}^{2+}$ . In addition to the characterization of EC behavior within the peptide-functionalized cryogels, cytokine/GF profile as well as redox state-related glutathione level in the cells were analyzed to elucidate some mechanisms of the peptide compositions.

## 2. Materials and methods

### 2.1. Materials

2-Hydroxyethyl methacrylate (HEMA), poly(ethylene glycol) diacrylate (PEGDA), *N,N,N',N'*-tetramethylethylenediamine (TEMED), ammonium persulfate (APS),  $\beta$ -cyclodextrin, acryloyl chloride, Fmoc-Gly-OH, Fmoc-Arg(Pbf)-OH, Fmoc-Asp(OtBu)-OH, Fmoc-His(Trt)-OH, Fmoc-Lys(Boc)-OH, Fmoc-6-aminohexanoic acid (Fmoc-Ahx), 1-

adamantaneacetic acid (Ada), Fmoc-Asp(OtBu)-O-Wang, Fmoc-Lys(Boc)-O-Wang, dansylglycine, 2-(1H-benzotriazol-1-yl)-1,1,3,3-tetramethyluronium hexafluorophosphate (HBTU), *N,N*-diisopropylethylamine (DIPEA), triisopropylsilane (TIPS), trifluoroacetic acid (TFA), *N,N*-dimethylformamide (DMF), dichloromethane (DCM) were purchased from Sigma-Aldrich, Alfa Aesar and Novabiochem.

Cell culture media and reagents were purchased from Paneco (Russia). 2-(4-amidinophenyl)-1H-indole-6-carboxamide (DAPI), phenazine methosulfate (PMS), polyethyleneimine (branched PEI,  $M_n \sim 10,000$ ) were purchased from Sigma Aldrich. 3-(4,5-dimethylthiazol-2-yl)-5-(3-carboxymethoxyphenyl)-2-(4-sulfophenyl)-2H-tetrazolium (MTS reagent) was purchased from Promega. Anti-VEGF (C-1) mouse monoclonal polyclonal antibody and phalloidin CruzFluor™ 647 conjugate were purchased from Santa Cruz Biotechnology. Donkey anti-mouse IgG (H + L) highly cross-adsorbed secondary antibody, Alexa Fluor 647 was obtained from Thermo Fisher. Reduced glutathione (GSH, purity 98%), oxidized glutathione (GSSG, purity 95%) and bovine serum albumin BSA were purchased from Acros Organics.

### 2.2. Solid phase synthesis of peptides

Ada-Ahx-GGRGD, Ada-Ahx-GGGHK and Ada-Ahx-GGK (dansylglycyl)GGHK peptides with C-terminal carboxyl group were synthesized on Fmoc-Asp(OtBu)-O-Wang and Fmoc-Lys(Boc)-O-Wang preloaded resins by Fmoc solid phase peptide synthesis method as described previously [28].

### 2.3. Preparation of cryogels

$\beta$ -Cyclodextrin-modified cryogels were synthesized by mixing of HEMA, PEGDA and acryloyl- $\beta$ -CD at a final concentration of 3.84% (v/v), 0.89% (v/v), and 0.24% (w/v) which, respectively, corresponded to 76.4, 19.0 and 4.6% of the total mass of all monomers. The crosslinking copolymerization was induced using 0.31% (w/v) ammonium persulfate and 0.40% (v/v) TEMED as initiator and activator of free radicals. The mixture was subsequently poured into a glass Petri dish, cooled at  $-12^\circ\text{C}$  for 4 h in a cooling thermostat and then kept at  $-18^\circ\text{C}$  for 24 h in freezer. The cryogel sheet was thawed and washed in milli-Q water at room temperature (RT).

### 2.4. Immobilization of peptides in cryogels

The cryogels were cut into 14 mm diameter circular discs, placed into 24-well plate and incubated at  $37^\circ\text{C}$  for 1 h under moderate agitation with aqueous solution of either Ada-Ahx-GGRGD or Ada-Ahx-GGK or their 1:1 mixture at a total peptide concentration of 0.36 mg/mL in each case. This concentration was shown to be saturated and corresponds to a calculated peptide loading of ca. 0.31 mg per  $1\text{ cm}^2$  of geometrical area of the cryogel [28]. To assess the incorporation and spatial distribution of peptide molecules in the cryogels, the materials were incubated under the same aforementioned conditions with dansyl-labeled GHK peptide, Ada-Ahx-GGK(dansylglycyl)GGK, followed by triple washing with PBS. The functionalized cryogel was then transversally cut and placed on a coverslip glass for its cross-sectional visualization. To analyze fluorescence profile lengthwise the diffusion front, the mean fluorescence intensity of dansyl-labeled peptide was recorded over 1.5 mm of depth from the cryogel top surface under laser excitation using LSM 780 Zeiss microscope. Zeiss Zen black software was used for data acquisition.

GHK-Cu complex was formed by treating the cryogel sheet having preimmobilized GHK peptide with  $\text{CuSO}_4$  ( $\text{Cu}^{2+}$ ) solution in excess concentration ( $C = 0.154\text{ mg/mL}$ ). Following 1 h incubation, non-chelated  $\text{Cu}^{2+}$  was removed by several washes with milli-Q water. For copper probing with PEI, the cryogels functionalized with GHK (0.18 or 0.36 mg/mL) as well as the peptide-free material were treated with  $\text{Cu}^{2+}$  and subsequently incubated with a solution of polyethyleneimine (PEI) (1 mg/mL) [29]. The color intensity of formed PEI- $\text{Cu}^{2+}$  complex was

visualized and compared with that of blank cryogel.

## 2.5. Scanning electron microscopy and elemental analysis

For scanning electron microscopy (SEM), the cryogels were freeze-dried and coated with 15 nm conductive layer (Au-Pd alloy) by cathode sputtering on a Q 150T ES sputter-coater (Quorum Technologies). The SEM analysis was carried out on a high-resolution field emission scanning electron microscope Merlin (Carl Zeiss) at an accelerating voltage of 5 kV and a probe current of 300 pA. The elemental characterization of the cryogels was performed by energy-dispersive X-ray spectroscopy (EDX) using a field emission scanning electron microscope (FE-SEM, Carl Zeiss).

## 2.6. Cell maintenance, seeding and proliferation

Human skin fibroblasts (HSF) were isolated as described in [30] and grown in  $\alpha$ -MEM supplemented with 10% FBS, penicillin (100 U/mL)/streptomycin (100  $\mu$ g/mL) and L-glutamine (2 mM). Primary freshly isolated human umbilical vein endothelial cells (HUVECs) were grown in RPMI 1640 supplemented with 20% FBS, penicillin (100 U/mL)/streptomycin (100  $\mu$ g/mL) and L-glutamine (2 mM), sodium pyruvate (2 mM), heparin (100  $\mu$ g/mL) and endothelial cell growth supplements (ECGS) in a temperature- and humidity-controlled incubator at 37 °C. Both types of cells were studied between passages 3 and 6. The culture medium was refreshed every 2 days.

The peptide-free cryogel as well as cryogels prefunctionalized with either RGD, GHK (GHK-Cu) or their mixture at a total peptide concentration of 0.36 mg/mL in each case were used as cell matrices. Prior to cell seeding, the materials were incubated in a soaking solution of penicillin (2.5 kU/mL)/streptomycin (2.5 mg/mL) antibiotic mixture for 1 h, rinsed with HBSS then preconditioned with 1 mL of culture medium. The cells suspended in serum-free medium were seeded onto cryogel surface using top seeding method in 24-well plate at a density of ca.  $2.9 \times 10^4$  cells/cm<sup>2</sup> of cryogel area and incubated for 1.5 h under standard culture conditions for attachment. To examine the effect of immobilized peptides on cell proliferative ability in the cryogels the MTS metabolic assay was used [31].

## 2.7. Cell adherence

To assess cell adhesion, HSFs were seeded on the top of control and peptide-functionalized cryogels in 24-well plate at a density of  $3.25 \times 10^4$  cells/cm<sup>2</sup>. Seeded cells were then allowed to adhere for 4 h in serum-free medium which was added at the level of the material surface to avoid cell washing down. Weakly-attached cells were subsequently collected after washing the cryogels with HBSS and counted to determine the amount of remaining adherent cells [32].

## 2.8. Immunocytochemistry

The cryogel matrices with cells were fixed with 4% *p*-formaldehyde at RT for 2.5 h and gently washed with PBS. After fixation, the samples were incubated in 0.1% Triton X-100 in PBS for 15 min for cell membrane permeabilization, followed by washing 3 times with PBS. Non-specific binding sites were blocked with 1.5% bovine serum albumin (BSA) for 30 min at RT. The samples were subsequently incubated with primary antibodies (1:500) against VEGF overnight at 4 °C, followed by incubation with Alexa Fluor 647-conjugated donkey anti-mouse secondary antibodies (1:350) for 45 min at RT. For cytoskeleton visualization, F-actin was labeled using phalloidin CruzFluor™ 647 conjugate ( $\lambda_{ex}$  and  $\lambda_{em}$  are 650 and 665 nm, respectively) in 1% BSA for 30 min at RT. Following washing in PBS, cell nuclei were stained using 4',6-diamidino-2-phenylindole (DAPI). The matrices were visualized by LSM 780 Zeiss microscope. Zeiss Zen black software was used for acquisition.

## 2.9. HPLC analysis for glutathione

Stock solutions of GSH and GSSG (10 mM) in 0.1% TFA were prepared. The analysis was carried out on a Dionex UltiMate 3000 HPLC system equipped with UV-Vis detector and a Kromasil C18 column. The eluent composition consisted of water/acetonitrile (95:5, v/v), 0.1% TFA and 12 mg/mL of sodium perchlorate NaClO<sub>4</sub>. An isocratic elution with a flow rate of 0.5 mL/min and detection wavelength of 215 nm was applied. The linear calibration graphs were obtained by plotting GSH and GSSG concentration (1–250  $\mu$ M) against the detected peak area.

For glutathione extraction, HUVECs were cultured within control cryogel and cryogels functionalized with peptides and copper complexes. In addition, some matrices were treated with CuSO<sub>4</sub> (C  $\approx$  0.5 mM), which was added to the culture medium at 24 h post-seeding and kept for another 24 h. At 48 h post-seeding, the matrices were washed and the cells were collected by trypsinization and counted to normalize cell density. The centrifuged cells were resuspended (at a cell density of ca.  $8.5 \times 10^5$  cells/mL) in 1% TFA used to precipitate proteins and maintain an acidic pH ( $\sim$ 2) to stabilize GSH in its reduced form, then briefly frozen at  $-80$  °C followed by thawing and 10-fold dilution with milli-Q water. The cell suspension was sonicated for 3 min on ice, then centrifuged at 13,000  $\times$ g for 12 min at 4 °C. The supernatants were then transferred into HPLC vials, injected and analyzed.

## 2.10. Multiplexed fluorescent bead-based immunoassay

Top-seeded HUVECs were grown within control and peptide-functionalized cryogels for 24 h. The conditioned medium aliquots were collected and the grown cells were subsequently harvested and lysed with IP buffer (25 mM Tris-HCl, pH 7.4, 0.5% Triton X-100, 150 mM NaCl, 5% glycerol, 1 mM EDTA with freshly added 1 mM p-APMSF). The cell culture medium and lysate were immediately frozen at  $-80$  °C. The analysis of secreted and cell-confined level of cytokines, respectively found in the medium and cell lysate samples, was performed using xMAP Luminex technology on a Bio-Plex MAGPIX analyzer (BioRad, USA) according to the manufacturer's recommendations. A commercially available MILLIPLEX MAP Human Cytokine/Chemokine Magnetic Bead Panel (HCYTMAP-60 K-PX41) was used to quantitatively measure cytokine/chemokine levels. The concentration of analytes in the samples was determined by their fluorescence intensities using a standard reference curve. Background levels of analytes in cell-free culture medium were subtracted from the concentrations of secreted factors in conditioned medium. Bio-Plex Manager 4.1 software (Bio-Rad Laboratories) was used to analyze the data.

## 2.11. Statistical analysis

Data were presented as mean  $\pm$  SD. Statistical significance was determined by one-way analysis of variance (ANOVA) followed by Tukey's Multiple Comparison post-test ( $*p < 0.05$ ,  $**p < 0.01$ ,  $***p < 0.001$ ).

## 3. Results and discussion

### 3.1. Cryogel design and characterization

#### 3.1.1. Peptide immobilization and copper complexation

$\beta$ -Cyclodextrin ( $\beta$ -CD)-containing pHEMA macroporous cryogel was synthesized by means of copolymerization of HEMA with acrylated derivatives of PEG and  $\beta$ -CD. It was used as an inert hydrogel scaffold subjected to in situ functionalization with adamantylated peptides.  $\beta$ -CD content in the modified material was earlier optimized to minimize the interference with pHEMA cryogel properties and to allow for peptide loading at ca. 0.31 mg per cm<sup>2</sup> of cryogel sheet [28]. The structures of RGD (1) and GHK (2) motif-containing peptides produced by solid-phase peptide synthesis is shown in Fig. 1A. The bioactive motifs were

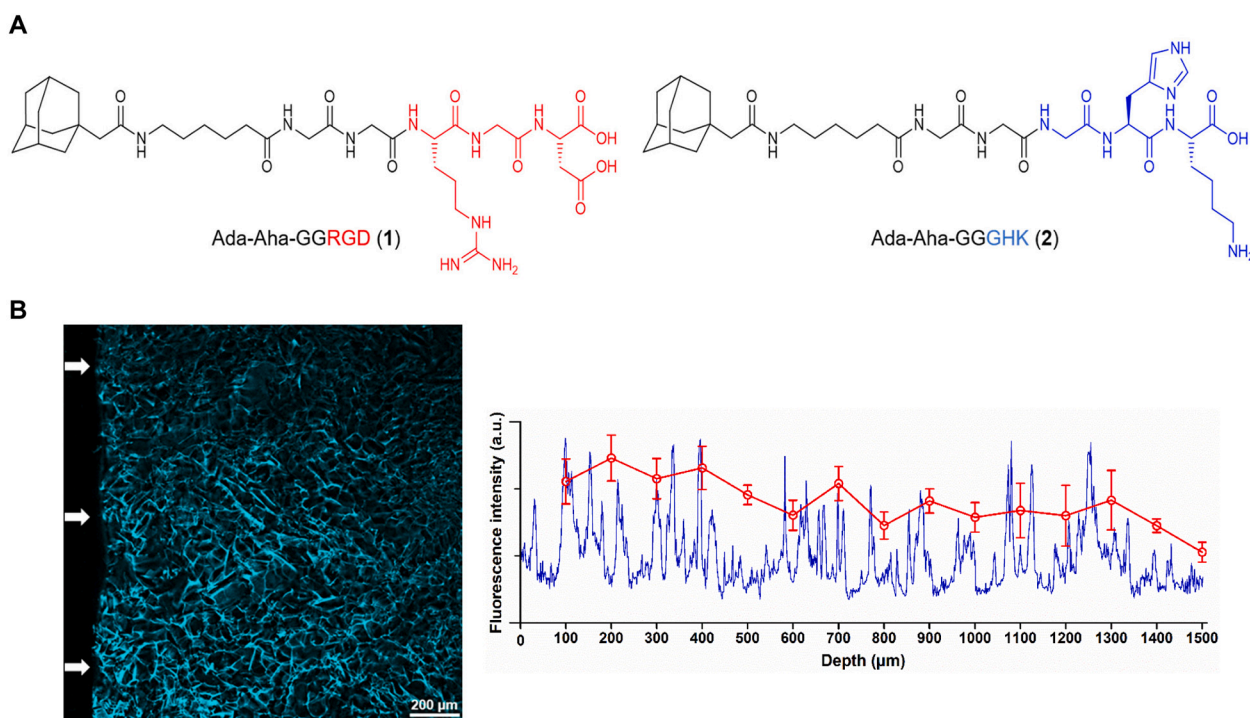


**Fig. 1.** A. The structures of synthesized adamantylated peptides: Ada-Ahx-GGRGD (1) and Ada-Ahx-GGGHK (2). B. LSCM image of cross-sectioned pHEMA- $\beta$ -CD cryogel functionalized with Ada-Ahx-GGK(dansylglycyl)GGHK and fluorescence intensity profile lengthwise diffusion front of peptide (arrows). Cryogel was incubated in peptide solution (0.36 mg/mL) for 1 h. Fluorescence profile (blue) was averaged for each 100  $\mu$ m distance (red curve, mean  $\pm$  SD). (For interpretation of the references to color in this figure legend, the reader is referred to the web version of this article.)

separated from the anchor adamantyl (Ad) group by a spacer consisting of aminohexanoic acid and glycines (Ahx-GG). Single adamantylated peptides and their composition can be effectively and stably immobilized in the modified cryogel by co-incubation leading to  $\beta$ -CD-Ad host-guest complex formation [28].

In this work, the penetration of adamantylated peptides into the cryogel was additionally characterized using fluorescently labeled Ada-Ahx-GGK(dansylglycyl)GGHK sequence. A 1.5 mm-thick  $\beta$ -CD-modified cryogel sheet was covered with the peptide solution (0.36 mg/mL), incubated for 1 h and cross-sectioned to analyze fluorescence profile lengthwise the diffusion front. The results demonstrated that the cryogel supports the bulk diffusion and continuous distribution of peptide molecules within the material (Fig. 1B).

Furthermore, the mean fluorescence signal persisted across the material to a depth up to 1300  $\mu$ m with only slight (less than 20%) decrease in average peptide content. Noticeable drop of the signal in underlying  $\sim$ 200  $\mu$ m layer was attributed to intrinsic anisotropy of the porous structure of cryogel bottom surface, which contains pores of smaller size (Fig. 1B). Such an anisotropy should not affect in vitro analysis since cultured mammalian cells generally inhabit upper layers of the cryogel sheet to a depth up to 1000  $\mu$ m [31]. These data confirm the effective immobilization of adamantylated peptides in  $\beta$ -CD-modified cryogel without significant gradient of bulk peptide content, which is expected for conventional hydrogels.

Immobilized GHK or RGD/GHK peptides were further combined with copper (II) ions by additional incubation of the functionalized cryogel with  $\text{CuSO}_4$  solution followed by washing out non-specifically attached  $\text{Cu}^{2+}$ . GHK peptide is known to form a high affinity coordination complex with  $\text{Cu}^{2+}$  with  $K_d = 7.0 \pm 1.0 \times 10^{-14}$  M [33].

Fig. 2 shows SEM data for freeze-dried pHEMA- $\beta$ -CD cryogel functionalized with GHK peptide,  $\text{Cu}^{2+}$  and their complex. The dried materials displayed a macroporous structure with interconnected pore architecture similar to that observed in the swollen state (Fig. 1B), both typical of cryogels. Such a structure facilitates solute exchange within

the bulk of cryogels as well as migration and functioning of mammalian cells in the materials [31,34]. Previously, the comparison of MTS reduction by the cells grown on culture plate surface and injected in cryogels suggested that these scaffolds caused only moderate ca. 1.5-fold retardation of MTS metabolization compared with cell monolayer [31]. The proposed procedure for peptide immobilization does not induce any morphological changes in pHEMA- $\beta$ -CD cryogel (Fig. 2). The immobilization via in situ affinity binding also allows avoiding side chemical modifications of the material that could be observed upon covalent attachment. Owing to their synthetic structure, the cryogel and peptide components are expected to have extended stability upon storage in comparison with natural ECM components, which is of practical importance for potential biomedical applications of the materials. As shown earlier, for research purposes the as-prepared peptide-functionalized cryogels can be stored in solution at least for 1 month with only slight decrease in the peptide content [28].

According to SEM images, the treatment of GHK-containing cryogel with  $\text{Cu}^{2+}$  resulted in brighter material surface indicating attachment of electron-dense component. The elemental analysis by peak area did not show significant increase in copper content in the peptide-free cryogel after incubation with  $\text{Cu}^{2+}$  (0.20 vs 0.23 wt%, Fig. 2). In the presence of GHK,  $\text{Cu}^{2+}$  was readily attached to the cryogel with a relative content of 1.92 and 3.79 wt% for the expected peptide loading of ca. 0.16 and 0.31 mg/cm<sup>2</sup>, respectively. This suggests that  $\text{Cu}^{2+}$  binds to GHK-containing cryogels almost in proportion to peptide loading ( $p < 0.001$ ), thus supporting the formation of stoichiometric GHK-Cu complex.

In addition, the materials were incubated with polyethylene imine, which forms a blue complex with  $\text{Cu}^{2+}$  [29]. The blue color intensity agreed well with SEM data further confirming complexation of  $\text{Cu}^{2+}$  with GHK-functionalized cryogels. Staining with PEI can be therefore used for the simple detection of copper ions in the cryogels.

Thus, the following variants of  $\beta$ -CD modified pHEMA cryogels were prepared, namely, the peptide-free control material (Ctrl) as well as materials functionalized with RGD, GHK, GHK-Cu, RGD/GHK, and

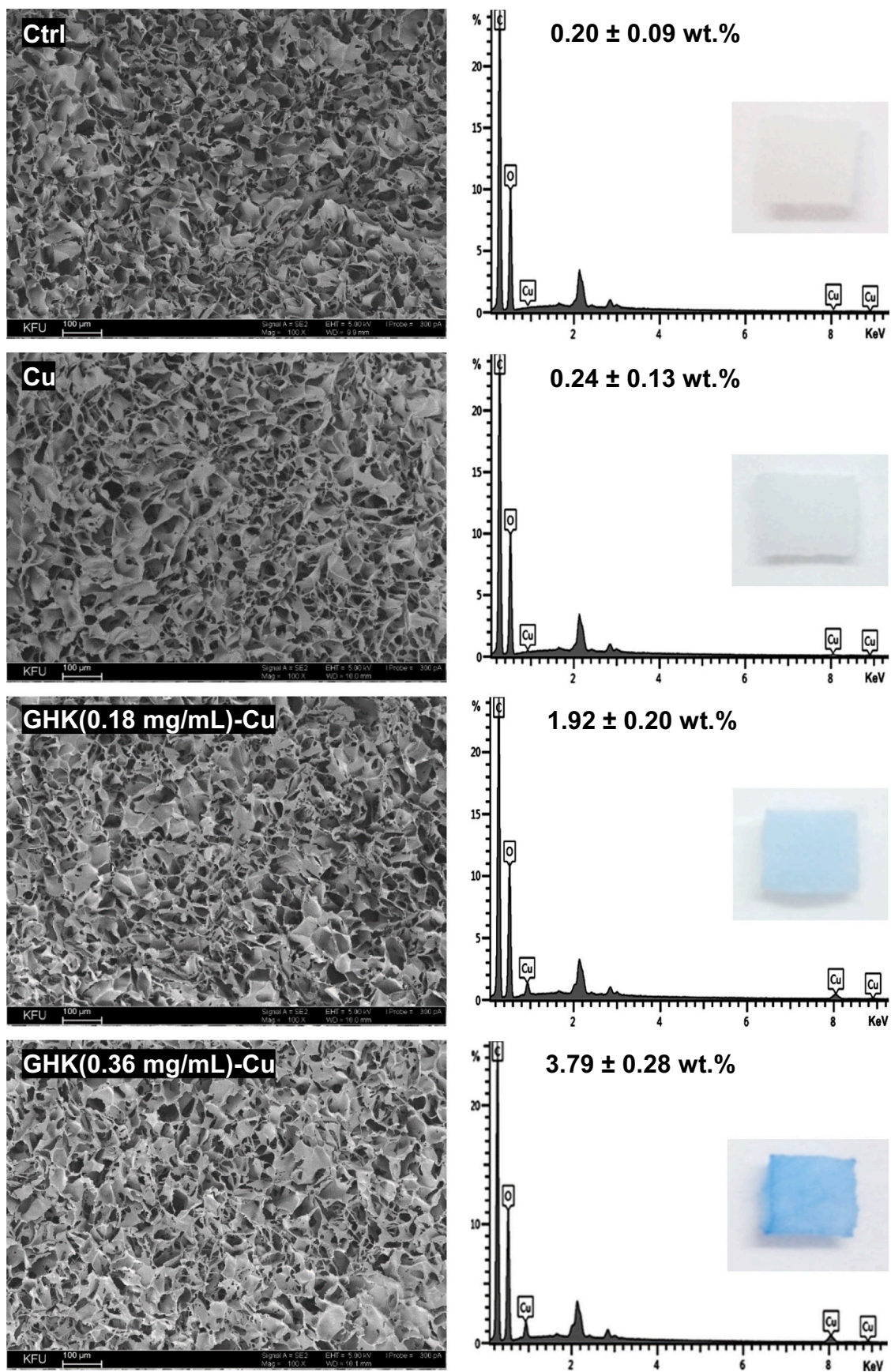


**Fig. 2.** SEM images (left panel) and element analysis data (right panel) for freeze-dried pHEMA- $\beta$ -CD cryogels treated with Ada-Ahx-GGGHK and/or  $\text{Cu}^{2+}$ . Pictures of corresponding PEI-stained materials are inserted in right panel. Materials were subsequently pre-incubated with peptide ( $C = 0.18$  or  $0.36$  mg/mL) and  $\text{CuSO}_4$  ( $C = 0.15$  mg/mL).

RGD/GHK-Cu components. The in vitro angiogenic effects of the functionalized cryogels were studied and compared.

### 3.1.2. Adhesion and proliferation of HSF

Early-passage human skin fibroblasts (HSF) were used as a standard primary cell model to evaluate cell adhesion and viability (proliferation) in contact with the peptide-functionalized cryogels. HSFs were top-seeded on the cryogel surface, and the adherence was assessed by calculating relative quantity of attached cells as a difference between the number of initially seeded cells and detached cells collected after cryogel washing (Fig. 3A). The results show that RGD peptide considerably supported cell attachment (68.3%) over peptide-free cryogel (28.5%), whereas GHK peptide and the copper complex caused relatively low promotion of cell adherence (39.8% and 36%, respectively). Similarly, GHK peptide augmented cell-adhesive effect of RGD peptide in dual composition (76.5%), and  $\text{Cu}^{2+}$  did significantly change the effect of composition (Fig. 3A).

Furthermore, top-seeded HSFs were allowed to grow within the cryogels for 72 h followed by their detection using the MTS metabolic assay [31,35]. The detected cell quantity/viability increased in the order: Ctrl < GHK  $\approx$  GHK-Cu < RGD < RGD/GHK < RGD/GHK-Cu (Fig. 3B). In particular, GHK and RGD peptides respectively caused an increase of the MTS signal by 1.40 and 3.07 times attributed to the promotion of both initial HSF adherence and subsequent proliferation in peptide-functionalized materials. According to these data, the combination of RGD with GHK noticeably increases HSF proliferation upon culturing within cryogels (compared with individual peptides) reaching an enhancement factor of 4.92, and  $\text{Cu}^{2+}$  somewhat augments the activity of composition (by 16%) (Fig. 3B).

These data also indicate that the immobilized copper component along with its stimulatory effect on cell proliferation does not cause cytotoxicity toward the primary human cells. The lack of cytotoxicity of  $\text{Cu}^{2+}$  within the functionalized cryogels was additionally confirmed by more prolonged 7-day culture of HSF (data not shown). The calculated content of immobilized  $\text{Cu}^{2+}$  was equivalent to a concentration in solution of  $\sim 0.48$  mM, at which free copper ions are expected to have

adverse effect on cells. Hence, the complexation with GHK peptide effectively prevents cytotoxicity of  $\text{Cu}^{2+}$  under experimental conditions in accordance with the earlier observation that even higher concentrations of GHK-Cu complex (up to 5.8 mM) were tolerated by keratinocytes [26].

Collectively, the results show that RGD motif based peptide provides superior cell-adhesive effect over GHK counterpart in the cryogel ECM model, in accordance with previous data for RGD peptides [14,36]. Nevertheless, immobilized GHK peptide caused a certain increase in HSF adherence by 8–11% (Fig. 3A). No promoting effect was earlier observed for human bone marrow-derived mesenchymal stem cells (MSCs) cultured on  $\text{G}_4\text{GHKSP}$  peptide-modified alginate hydrogel [37]. This may suggest that the designed synthetic cryogel matrix provides more specific cellular response to immobilized peptides. Furthermore, co-immobilization of RGD and GHK peptides in this matrix dramatically promotes proliferation/viability of HSFs. The complexation of copper with GHK or RGD/GHK does not inhibit HSF adhesion and proliferation, while slightly stimulates the latter process in the case of peptide composition (Fig. 3).

## 3.2. Angiogenic properties of peptide-functionalized cryogels

### 3.2.1. Proliferation of HUVEC

HUVEC primary cells were used as a relevant in vitro model to characterize angiogenic potential of biomaterials [38]. Top-seeded cells were cultured in the peptide-functionalized cryogels for 72 h and subjected to the MTS assay. The peptides induced defined promoting effect on HUVEC proliferation/viability, which clearly increased in the order: Ctrl < GHK < GHK-Cu < RGD < RGD/GHK < RGD/GHK-Cu (Fig. 4). These results generally correlated with those for HSF, however, in the case of HUVEC a profound effect of the copper complex was observed. In particular,  $\text{Cu}^{2+}$  increased the MTS signal for GHK- and RGD/GHK-functionalized materials by 36–56% ( $*p < 0.05$ ). This shows increased responsiveness of HUVEC to  $\text{Cu}^{2+}$  (GHK-Cu complex) in accordance with established angiogenic activity of this microelement in biomaterials [39].

Earlier, SPARC (secreted protein acidic and rich in cysteine) fragments (SPARC<sub>113</sub> and SPARC<sub>118</sub> peptides) were introduced to PEG hydrogel to confer angiogenic properties [40]. The SPARC peptides contain GHK sequence which may determine their bioactivity. Altogether, the results support the relevance of using GHK derivatives and complexes for biomaterials development and encourage further characterization of angiogenesis-related effects of the peptides.

### 3.2.2. Morphology of HUVEC

The formation of new tubular structures requires the differentiation of ECs to a specialized morphologically altered cell phenotype [10]. To characterize HUVEC morphology in the functionalized cryogels the cells were stained for F-actin with fluorescently labeled phalloidin.

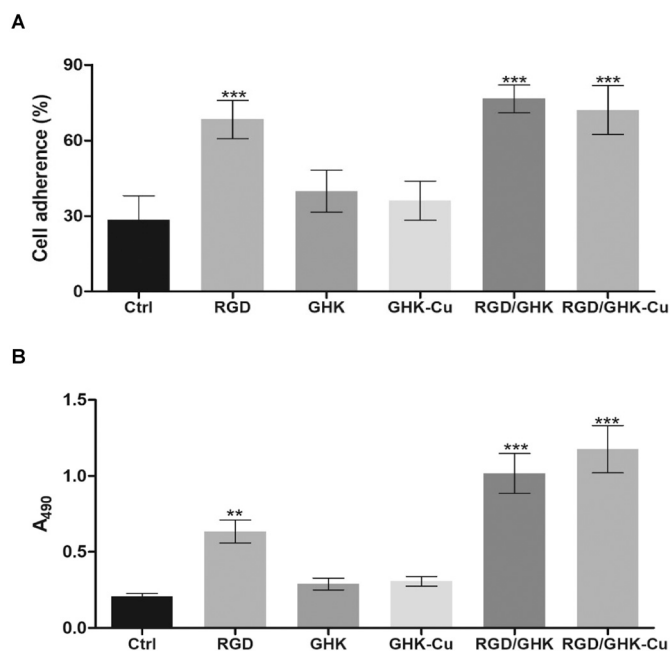


Fig. 3. A. HSF adherence on surface of peptide-functionalized pHEMA- $\beta$ -CD cryogels after 4 h incubation (% of the total cell number). B. HSF viability determined using MTS assay at day 3 post-seeding on peptide-functionalized pHEMA- $\beta$ -CD cryogels. The data are presented as mean  $\pm$  SD ( $n = 3$ ,  $**p < 0.01$ ,  $***p < 0.001$ ).

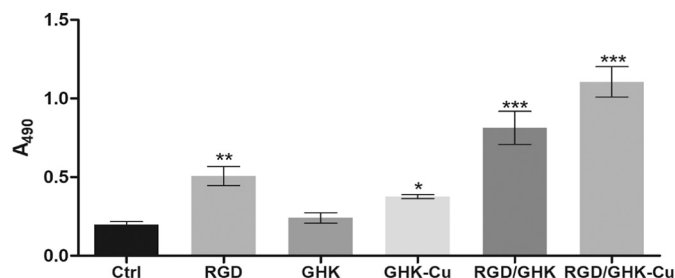


Fig. 4. Effect of immobilized RGD and GHK (GHK-Cu) peptides on proliferation/viability of HUVEC in peptide-functionalized pHEMA- $\beta$ -CD cryogels. MTS signal was detected at day 3 post-seeding. Control (Ctrl) refers to non-functionalized cryogel. The data are presented as mean  $\pm$  SD ( $n = 3$ ,  $*p < 0.05$ ,  $**p < 0.01$ ,  $***p < 0.001$ ).

In the absence of peptides, HUVECs were characterized by low adherence and spreading on the material surface and had round cell morphology lacking sprouts (Fig. 5A, Ctrl). Noticeable morphological changes of HUVECs were induced by immobilized GHK and more profoundly GHK-Cu (Fig. 5A). However, the cells still showed a relatively low density attributed to weak adhesive effect of GHK peptide. RGD peptide alone, though increased the cell density in accordance with the MTS assay data (Fig. 4), weakly affected cell morphology (Fig. 5A).

Combination of RGD with GHK and especially GHK-Cu further increased cell number and dramatically rearranged cell morphology on the cryogel surface. In particular, in the case of RGD/GHK-Cu composition, HUVECs were more elongated and gave extended sprouts to reach out neighbor cells, thus establishing cellular connections. The cells tended to form circular tubule-like structures, however, their detection at highly porous cryogel support by LSCM was complicated compared

with flat surfaces. The semitransparent structure of cryogels [28,31] allowed to additionally analyze cresyl violet stained cells on the material surface using bright-field microscopy (Fig. 5B), which confirmed profoundly increased density of the cells grown in (RGD/GHK-Cu)-functionalized cryogel compared with peptide-free material. Furthermore, well distinguished circular cell ensembles attributed to primitive tubular structures were detected throughout the former matrix (Fig. 5B). At least one such ensemble with mean inner area of  $1654.4 \pm 438.4 \mu\text{m}^2$  was detected per  $\text{mm}^2$  of cryogel surface. The above observations underlie inducible dynamic alterations in ECs to mediate tubulogenesis.

Altogether, these results demonstrate the crucial role of triple RGD/GHK-Cu composition in promoting the angiogenic activity of the cryogels toward HUVECs (Fig. 5). Whereas mitogenic effect is mainly provided by RGD/GHK (Fig. 4), the presence of  $\text{Cu}^{2+}$  is apparently required to induce morphological changes attributed to angiogenic cell

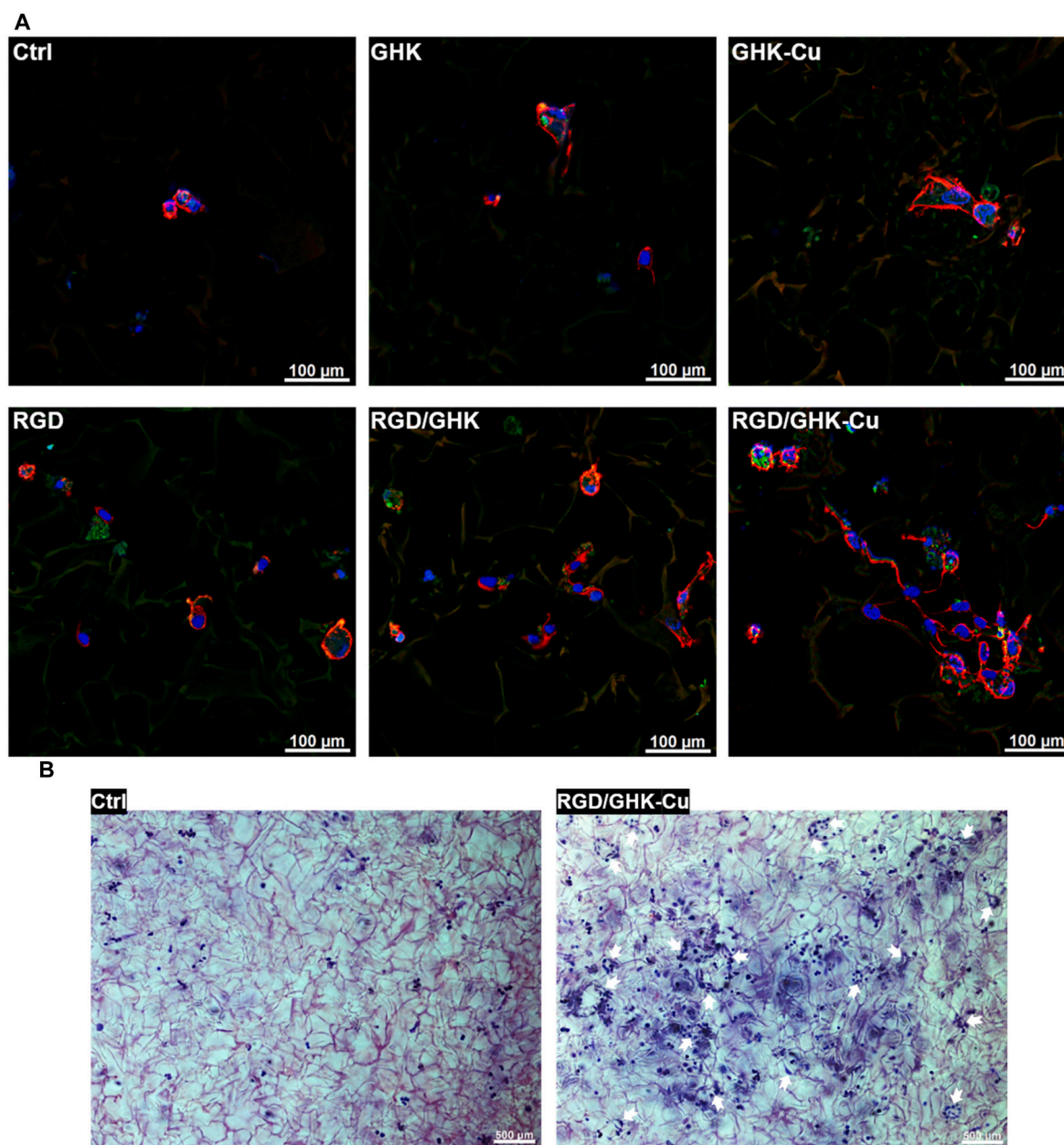


**Fig. 5.** A. Representative LSCM images of HUVECs grown in peptide-functionalized pHEMA-β-CD cryogels at 48 h post-seeding. Cells were stained with phalloidin CruzFluor™ 647 conjugate for F-actin (red) and DAPI for nuclei (blue). B. Representative bright-field microscopy images of HUVECs stained with cresyl violet at 48 h post-seeding in peptide-free (Ctrl) and (RGD/GHK-Cu)-functionalized pHEMA-β-CD cryogels. (For interpretation of the references to color in this figure legend, the reader is referred to the web version of this article.)

differentiation [39,41].

### 3.3. Glutathione level in HUVEC

Glutathione (GSH) is prevailing antioxidant in mammalian cells with vital protective and regulatory functions. The balance between redox forms of GSH is a key parameter of redox homeostasis, which controls cell proliferation, differentiation and programmed death via different redox sensitive transcriptional factors and enzymes [42]. Therefore, relationships between intracellular GSH level and regenerative effects of peptides may provide additional insight into their mechanisms of action.

Relative content of GSH in HUVECs cultured in peptide-functionalized cryogels was analyzed by HPLC (Fig. 6). It was found that GHK unlike RGD induced noticeable increase in GSH level by 21%. The effect of GHK could be associated with its cell-modulating activities potentially involving change in cell redox state, e.g. via complexing transition metals and promoting antioxidant biosynthesis [20]. RGD peptide, acting as an ECM cytoadhesive motif, should induce adherence-related cellular events [15], which probably do not directly affect GSH biosynthesis. However, cell responses to RGD and GHK peptides seem to be interconnected as RGD/GHK composition caused double increase in GSH level (by 41.5%) compared with GHK alone (Fig. 6).

Supplementation of free 0.5 mM  $\text{Cu}^{2+}$  to the culture medium (24 h post-seeding the cells) resulted in more than 2-fold decrease in the GSH signal when the cells were cultured in peptide-free cryogel (Fig. 6). These data are explained by prooxidant action of copper (II) ions, which involves Fenton-like reaction [43] and redox cycling with biomolecules [42,44] to produce reactive oxygen species (ROS) eliminated at the expense of GSH. The prooxidant effect of supplemented  $\text{Cu}^{2+}$  was much lower when (RGD/GHK)-functionalized cryogel was used (Fig. 6). This could be attributed to the ability of peptides to both increase GSH level in HUVECs and bind copper ions (primarily, by GHK sequence), resulting in the capture of  $\text{Cu}^{2+}$  from culture medium by the functionalized cryogel. Histidine residue is known to be a key ligand for  $\text{Cu}^{2+}$  and other transition metals [45], allowing GHK and other histidine-containing peptides to complex the metals and modulate their cellular transportation/availability [25]. The complexation can also minimize side reactions and cytotoxicity of these metals associated with oxidative stress [26]. GHK is regarded as a carrier system for  $\text{Cu}^{2+}$ , which allows for the peptide receptor-mediated uptake of  $\text{Cu}^{2+}$  (GHK-Cu) by mammalian cells. Inside the cells, GHK-Cu can activate different regenerative and protective genes [25].

When  $\text{Cu}^{2+}$  was pre-complexed with both GHK and RGD/GHK and not provided in the culture medium, it abolished the increasing effect of the peptides on GSH level in cells but did not decrease it in comparison with the control level detected in cells grown without effectors (Fig. 6).

Altogether, the results suggest that GHK, RGD/GHK and their complex with  $\text{Cu}^{2+}$  induce variation in GSH content and hence redox balance in HUVECs which probably underlies the stimulation of cell

proliferation (Fig. 4) and angiogenic responses (Fig. 5) by these factors. It could be supposed that the proliferation phase is accompanied by the increase in metabolic activity and GSH level in the cells whereas the initiation of their angiogenic differentiation involves some decrease in GSH pool. The variation in GSH content may occur in response to physiological production of ROS, which act as secondary messengers in angiogenic pathways via regulation of HIF1- $\alpha$  and VEGF expression [46,47]. In excess concentration,  $\text{Cu}^{2+}$  may elevate ROS above physiological levels which are harmful for microtubular structures [48], whereas its binding to GHK peptide permits to avoid toxic levels, providing conditions for cell differentiation [25,27].

### 3.4. Analysis of angiogenic cytokines and growth factors

ECs are known to be a major source of FGF-2 [49], IL-8 [50], IL-6 [51], VEGF [52] and MCP-1 [53] as well as other factors involved in both their autocrine regulation and the recruitment of other cells to support neovascularization. The expression of these cytokines can be modulated in the presence of oxygen supply or ROS production with participation of HIF-1 $\alpha$  and HIF-2 $\alpha$  transcriptional factors [54] both known to upregulate VEGF biosynthesis [55]. A continuous expression of endogenous VEGF in mature ECs is necessary to maintain vascular integrity, cell viability and metabolism [56].

The profile of cytokines/chemokines and essential GFs in HUVECs cultured within peptide-functionalized cryogels was analyzed using Bio-Plex multiplex immunoassay. Fig. 7A, B shows the level of some key cytokines and GFs such as FGF-2, VEGF, IL-6, IL-8, MCP-1 with established roles in tissue regeneration and angiogenesis; extended cytokines profile is provided in Fig. 7C. All variants of individual and combined peptides were found to induce upregulation of the analyzed factors both in the cell culturing medium (Fig. 7A) and cell lysate (Fig. 7B). Among individual peptides, GHK-Cu showed increased promoting effect on the secretion of FGF-2 (3.4-fold,  $*p < 0.05$ ) and its intracellular level (3.6-fold,  $*p < 0.05$ ). The combination of GHK or GHK-Cu with RGD induced further increase in the extracellular level of FGF-2 by 4.1- and 4.8-fold ( $**p < 0.01$ ), respectively.

Similar profile was detected for secreted VEGF, e.g. with 3.3- and 4.7-fold increase in this factor content by GHK-Cu and RGD/GHK-Cu, respectively. Likewise, a significant upregulation of IL-6, IL-8 and MCP-1 was induced by RGD/GHK-Cu ( $*p < 0.05$ ), which elevated both extra- and intracellular levels of these cytokines by 2.5–9.7 times (Fig. 7).

Considering VEGF as a key regulator of blood vessels formation and functioning, we additionally visualized expression and distribution of this marker in HUVEC-cultured matrices (Fig. 8). (GHK-Cu)-functionalized cryogel, unlike control and GHK-functionalized ones, was found to promote VEGF biosynthesis by HUVEC. The immunofluorescence intensity for VEGF in the cells was significantly enhanced in the presence of RGD/GHK-Cu compared with RGD/GHK, which showed lower VEGF

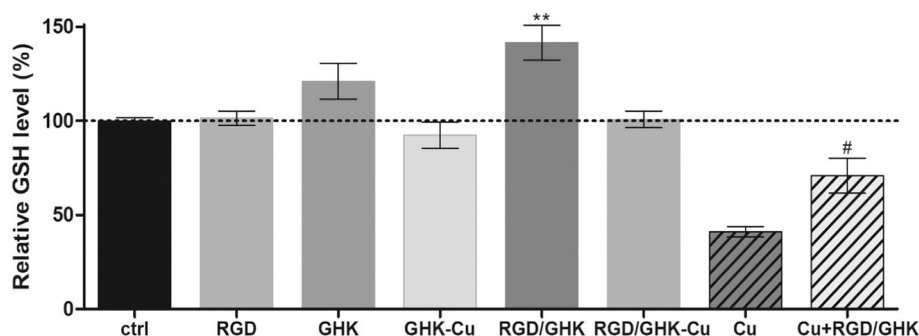
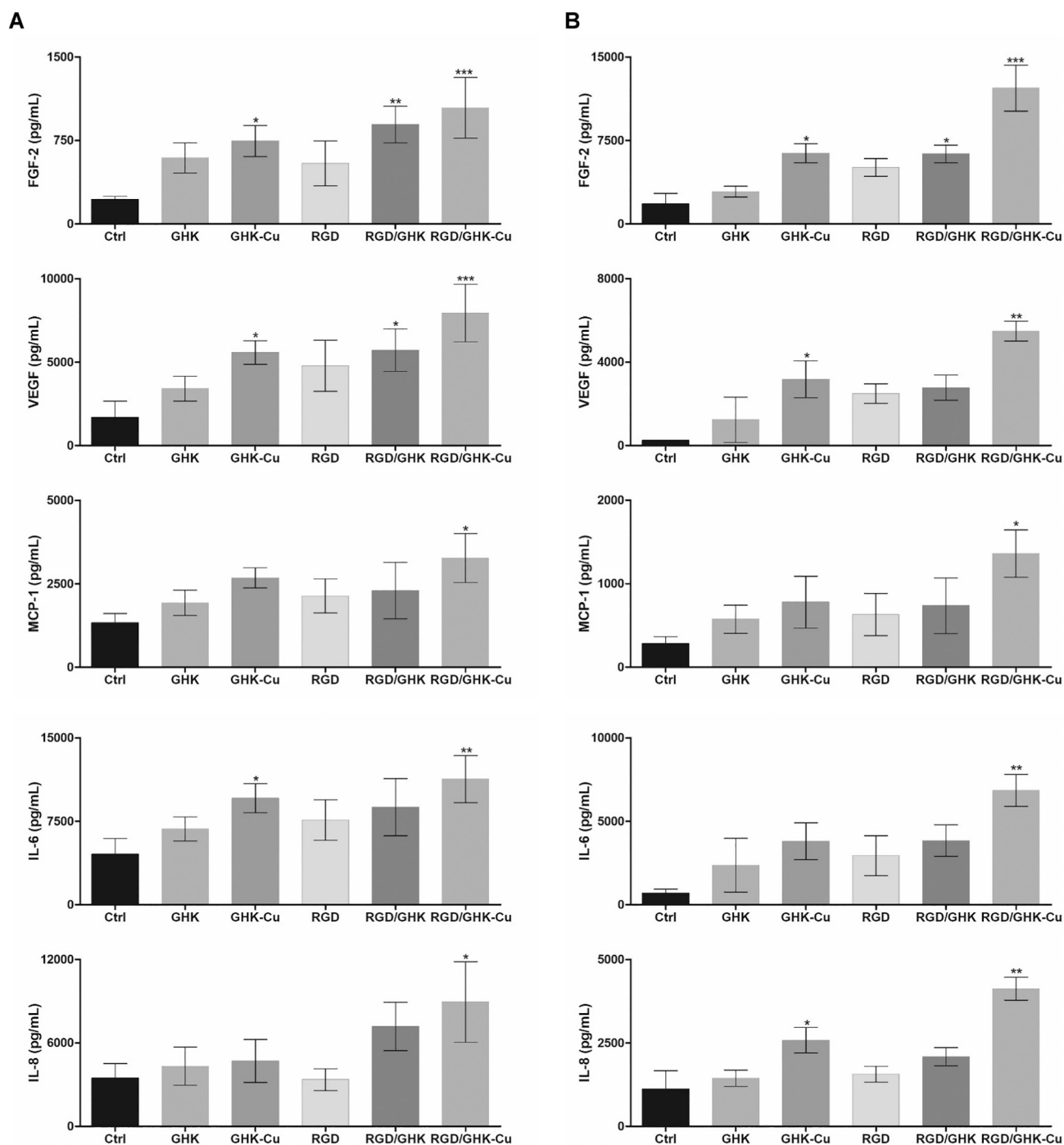


Fig. 6. Relative GSH level in HUVECs grown in peptide-functionalized pHEMA- $\beta$ -CD cryogels at 48 h post-seeding. The signal was normalized per cell number and is shown in % relative to control GSH level (100%). For hashed columns, cells were treated for 24 h with 0.5 mM  $\text{CuSO}_4$  added to culture medium at 24 h post-seeding. The data are presented as mean  $\pm$  SD ( $n = 3$ ),  $**p < 0.01$  (vs. Ctrl),  $\#p < 0.05$  (vs. Cu).



**Fig. 7.** Analysis of cytokines and growth factors in cell culture medium (A) and lysates (B) of HUVECs cultured on peptide-functionalized pHEMA- $\beta$ -CD cryogels at 24 h post-seeding. The data are presented as mean  $\pm$  SD ( $n = 3$ , \* $p < 0.05$ , \*\* $p < 0.01$ , \*\*\* $p < 0.001$ ). C. Radar plot representation of extended profile in cell culture medium (left chart) and lysate (right chart); log concentrations (pg/mL) are indicated.

expression in cytosol (Fig. 8) in agreement with the multiplex assay.

It was previously shown that enhanced liposomal delivery of GHK-Cu into HUVECs promoted cell proliferation and VEGF and FGF-2 expression compared with unformulated GHK-Cu [41], suggesting intracellular mode of action of the complex. Stimulating effect of GHK covalently immobilized in alginate HM on VEGF secretion by human bone marrow-derived MSCs [37] and osteogenic differentiation of umbilical cord blood MSCs [57] could be also mediated by the peptide binding to integrin  $\beta 1$ , yet GHK did not support MSC adhesion [37]. The interaction of GHK with cell membrane receptor(s), however, should not

exclude its uptake by the cells in accordance with evidence on the ability of GHK-Cu to penetrate across cell membranes and human skin [58,59].

Both cellular binding and uptake of GHK could be potentially promoted by co-immobilized cell-adhesive RGD, and this may provide additional mechanism for enhanced effects of dual peptide compositions (Figs. 4, 5, 6, 7).

Collectively, the results for the first time show that the combination of synthetic affinity-immobilized RGD and GHK peptides synergistically enhances the production of proangiogenic factors by ECs grown in the cryogel ECM model. Moreover, the specific complexation of this

C

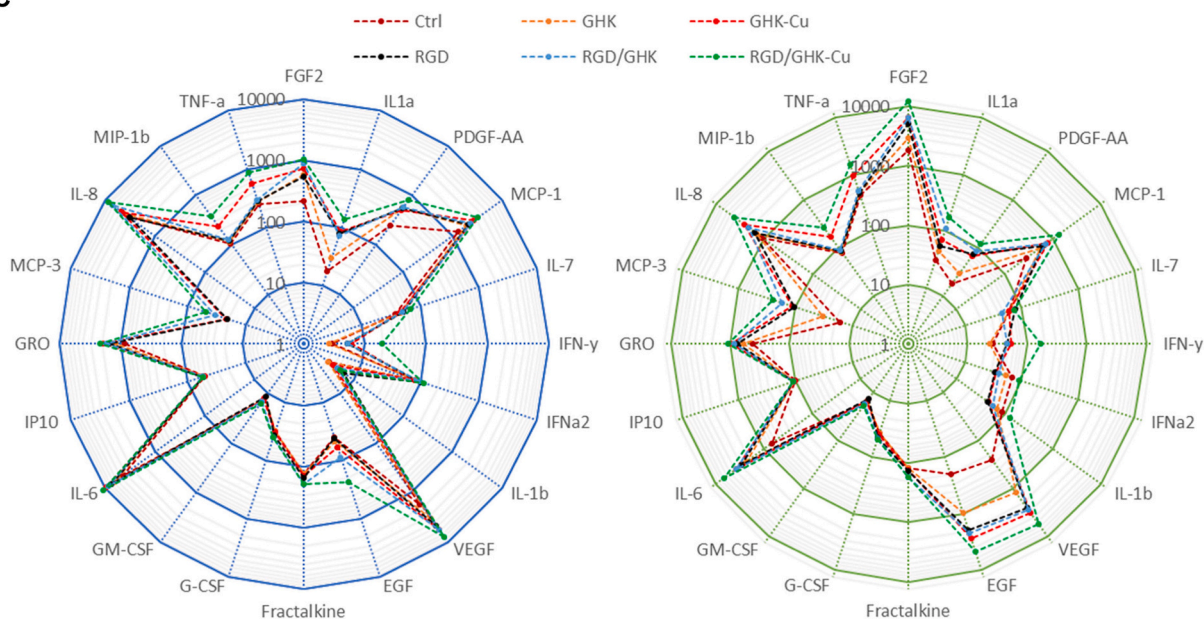


Fig. 7. (continued).

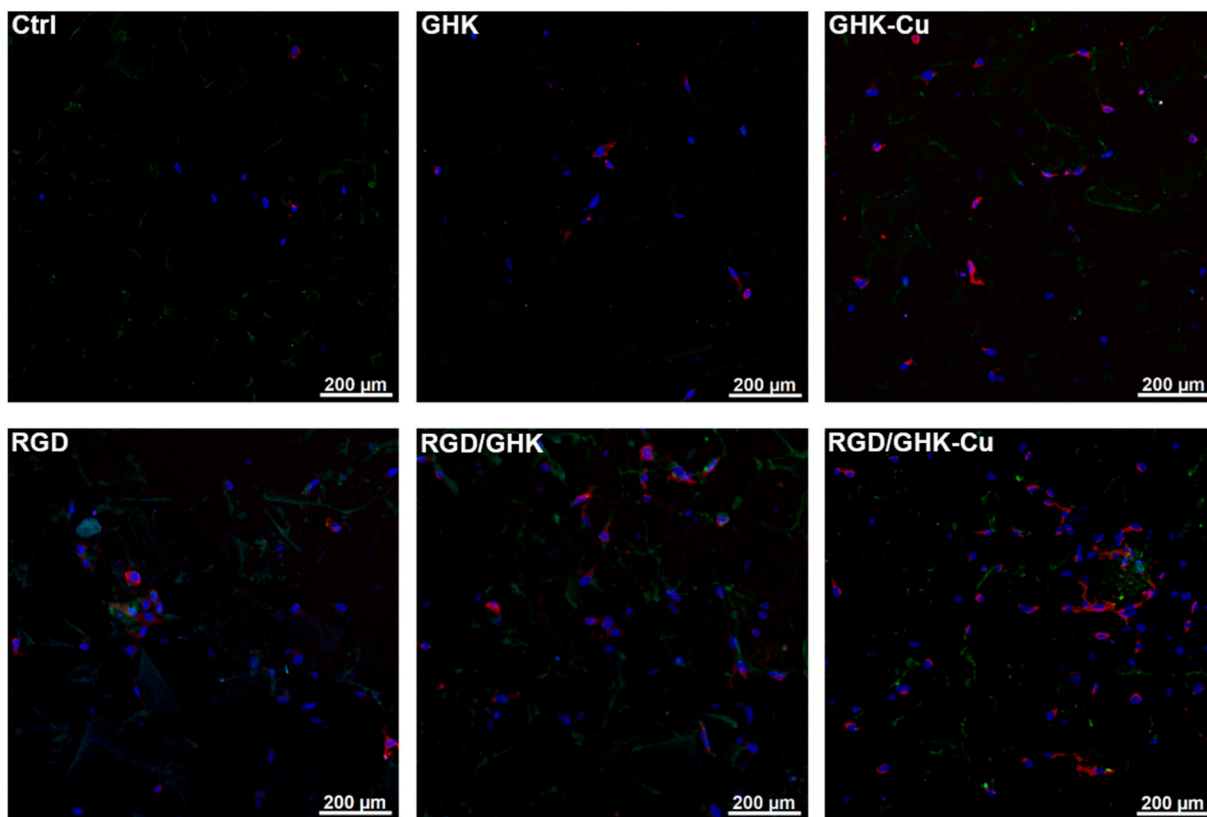


Fig. 8. Immunofluorescence detection of VEGF in HUVECs at 24 h post-seeding on top surface of peptide-functionalized pHEMA- $\beta$ -CD cryogels. Corresponding DAPI-stained nuclei are shown.

composition with copper ions insures more profound and robust stimulating effect on key cytokine and GF levels (Figs. 7 and 8) in addition to that on the proliferation and morphological differentiation of HUVECs in the matrix. Therefore, RGD/GHK-Cu triple composition is expected to be a powerful stimulator of angiogenesis both in vitro and in vivo and a potential alternative to natural GFs. The composition can be stably

immobilized in both synthetic and natural polymer-derived HMs using different chemical strategies. Natural polymers with native bioactive sequences and of biodegradable nature are expected to further contribute to regenerative activity of the peptides; corresponding composite biomaterials could be of practical interest in different therapeutic applications.

#### 4. Conclusions

In this study, pHEMA-PEG- $\beta$ -CD cryogels were functionalized with adamantylated RGD, GHK, and GHK-Cu peptides in a highly efficient manner to construct a synthetic ECM model. This model was shown to provide informative assessment of short peptides, active metals and their compositions as promising bioinductive components of tissue regenerating and engineering materials. The combination of two simplest peptide motifs, i.e. RGD and GHK, greatly enhances various in vitro angiogenic responses to the materials, and additional complexation of GHK with  $\text{Cu}^{2+}$  ensures even greater effects, which are probably associated with redox modulating activity of GHK-Cu. We believe, based on our results and some existing data, that regenerative effects of biomaterials can be substantially improved by the evolution of biochemical structure and spatial organization of peptide molecules and using active metals to form coordination compounds with the peptides. The results encourage further discovery of oligopeptide based therapeutic compositions using the cryogel model as well as the development of bioinductive materials loaded with the identified RGD/GHK-Cu triple system.

#### CRedit authorship contribution statement

**M. Zoughaib:** Writing - Original Draft, Investigation, Methodology.  
**Duong Luong:** Investigation. **Ruslan Garifullin:** Investigation. **Dilara Z. Gatina:** Investigation. **Svetlana V. Fedosimova:** Investigation.  
**Timur I. Abdullin:** Conceptualization, Writing - Review & Editing, Supervision.

#### Declaration of competing interest

The authors declare that they have no known competing financial interests or personal relationships that could have appeared to influence the work reported in this paper.

#### Acknowledgments

This work was funded by RFBR (Grant 19-03-01010) and performed according to the Russian Government Program of Competitive Growth of Kazan Federal University (KFU). M. Zoughaib and R. Garifullin acknowledge Russian Science Foundation project No 20-73-10105 (peptide synthesis and characterization). The authors greatly acknowledge Dr. Ilnur Salafutdinov (Interdisciplinary Centre for Shared Use of KFU) for providing HUVECs and assistance with multiplex analysis, Yu. Osin and V. Vorobev (Interdisciplinary Center for Analytical Microscopy of KFU) for microscopy analysis.

#### References

- [1] K. Bootsma, M.M. Fitzgerald, B. Free, E. Dimbath, J. Conjerti, G. Reese, D. Konkolewicz, J.A. Berberich, J.L. Sparks, 3D printing of an interpenetrating network hydrogel material with tunable viscoelastic properties, *J. Mech. Behav. Biomed. Mater.* 70 (2017) 84–94, <https://doi.org/10.1016/j.jmbm.2016.07.020>.
- [2] E.C. Chan, S.M. Kuo, A.M. Kong, W.A. Morrison, G.J. Dusting, G.M. Mitchell, S. Y. Lim, G.S. Liu, Three dimensional collagen scaffold promotes intrinsic vascularisation for tissue engineering applications, *PLoS One* 11 (2016), e0149799, <https://doi.org/10.1371/journal.pone.0149799>.
- [3] Y.H. Choi, S.H. Kim, I.S. Kim, K. Kim, S.K. Kwon, N.S. Hwang, Gelatin-based microhydrogel carrying genetically engineered human endothelial cells for neovascularization, *Acta Biomater.* 95 (2019) 285–296, <https://doi.org/10.1016/j.actbio.2019.01.057>.
- [4] Y. Duan, X. Li, X. Zuo, T. Shen, S. Yu, L. Deng, C. Gao, Migration of endothelial cells and mesenchymal stem cells into hyaluronic acid hydrogels with different moduli under induction of pro-inflammatory macrophages, *J. Mater. Chem. B* 7 (2019) 5478–5489, <https://doi.org/10.1039/c9tb01126a>.
- [5] A.A. Ucuozan, D.V. Bufalino, Y. Pang, H.P. Greisler, Angiogenic endothelial cell invasion into fibrin is stimulated by proliferating smooth muscle cells, *Microvasc. Res.* 90 (2013) 40–47, <https://doi.org/10.1016/j.mvr.2013.06.012>.
- [6] A.K. Ekaputra, G.D. Prestwich, S.M. Cool, D.W. Huttmacher, The three-dimensional vascularization of growth factor-releasing hybrid scaffold of poly (epsilon-caprolactone)/collagen fibers and hyaluronic acid hydrogel, *Biomaterials.* 32 (2011) 8108–8117, <https://doi.org/10.1016/j.biomaterials.2011.07.022>.
- [7] L.L. Chiu, M. Radisic, Scaffolds with covalently immobilized VEGF and angiotensin-1 for vascularization of engineered tissues, *Biomaterials.* 31 (2010) 226–241, <https://doi.org/10.1016/j.biomaterials.2009.09.039>.
- [8] K.G. Sreejalekshmi, P.D. Nair, Biomimeticity in tissue engineering scaffolds through synthetic peptide modifications-altering chemistry for enhanced biological response, *J. Biomed. Mater. Res. A* 96 (2011) 477–491, <https://doi.org/10.1002/jbm.a.32980>.
- [9] K.J. Lampe, S.C. Heilshorn, Building stem cell niches from the molecule up through engineered peptide materials, *Neurosci. Lett.* 519 (2012) 138–146, <https://doi.org/10.1016/j.neulet.2012.01.042>.
- [10] S. Ali, J.E. Saik, D.J. Gould, M.E. Dickinson, J.L. West, Immobilization of cell-adhesive laminin peptides in degradable PEGDA hydrogels influences endothelial cell tubulogenesis, *Biores. Open Access.* 2 (2013) 241–249, <https://doi.org/10.1089/biores.2013.0021>.
- [11] J. Zhu, Bioactive modification of poly(ethylene glycol) hydrogels for tissue engineering, *Biomaterials.* 31 (2010) 4639–4656, <https://doi.org/10.1016/j.biomaterials.2010.02.044>.
- [12] R. Cruz-Acuna, A.J. Garcia, Synthetic hydrogels mimicking basement membrane matrices to promote cell-matrix interactions, *Matrix Biol.* 57–58 (2017) 324–333, <https://doi.org/10.1016/j.matbio.2016.06.002>.
- [13] S.S. Ho, K.C. Murphy, B.Y. Binder, C.B. Vissers, J.K. Leach, Increased survival and function of mesenchymal stem cell spheroids entrapped in instructive alginate hydrogels, *Stem Cells Transl. Med.* 5 (2016) 773–781, <https://doi.org/10.5966/sctm.2015-0211>.
- [14] J. Jia, R.C. Coyle, D.J. Richards, C.L. Berry, R.W. Barrs, J. Biggs, C. James Chou, T. C. Trusk, Y. Mei, Development of peptide-functionalized synthetic hydrogel microarrays for stem cell and tissue engineering applications, *Acta Biomater.* 45 (2016) 110–120, <https://doi.org/10.1016/j.actbio.2016.09.006>.
- [15] G.C. Ingavle, S.H. Gehrke, M.S. Detamore, The bioactivity of agarose-PEGDA interpenetrating network hydrogels with covalently immobilized RGD peptides and physically entrapped aggrecan, *Biomaterials.* 35 (2014) 3558–3570, <https://doi.org/10.1016/j.biomaterials.2014.01.002>.
- [16] Y.H. Yang, Z. Khan, C. Ma, H.J. Lim, L.A. Smith Callahan, Optimization of adhesive conditions for neural differentiation of murine embryonic stem cells using hydrogels functionalized with continuous Ile-Lys-Val-Ala-Val concentration gradients, *Acta Biomater.* 21 (2015) 55–62, <https://doi.org/10.1016/j.actbio.2015.04.031>.
- [17] T. Ren, S. Yu, Z. Mao, S.E. Moya, L. Han, C. Gao, Complementary density gradient of poly(hydroxyethyl methacrylate) and YIGSR selectively guides migration of endothelial cells, *Biomacromolecules.* 15 (2014) 2256–2264, <https://doi.org/10.1021/bm500385n>.
- [18] M.H. Fittkau, P. Zilla, D. Bezuidenhout, M.P. Lutolf, P. Human, J.A. Hubbell, N. Davies, The selective modulation of endothelial cell mobility on RGD peptide containing surfaces by YIGSR peptides, *Biomaterials.* 26 (2005) 167–174, <https://doi.org/10.1016/j.biomaterials.2004.02.012>.
- [19] F.X. Maquart, J.C. Monboisse, Extracellular matrix and wound healing, *Pathol. Biol. (Paris)* 62 (2014) 91–95, <https://doi.org/10.1016/j.patbio.2014.02.007>.
- [20] L. Pickart, J.M. Vasquez-Soltero, A. Margolina, GHK peptide as a natural modulator of multiple cellular pathways in skin regeneration, *Biomed. Res. Int.* 2015 (2015) 648108, <https://doi.org/10.1155/2015/648108>.
- [21] S. Sharma, A. Dua, A. Malik, Biocompatible stimuli responsive superabsorbent polymer for controlled release of GHK-Cu peptide for wound dressing application, *J. Polym. Res.* 24 (2017) 104, <https://doi.org/10.1007/s10965-017-1254-z>.
- [22] A. Bhattacharjee, K. Chakraborty, A. Shukla, Cellular copper homeostasis: current concepts on its interplay with glutathione homeostasis and its implication in physiology and human diseases, *Metallomics.* 9 (2017) 1376–1388, <https://doi.org/10.1039/c7mt00066a>.
- [23] H. Xie, Y.J. Kang, Role of copper in angiogenesis and its medicinal implications, *Curr. Med. Chem.* 16 (2009) 1304–1314, <https://doi.org/10.2174/092986709787846622>.
- [24] D.C. Rigracciolo, A. Scarpelli, R. Lappano, A. Pisano, M.F. Santolla, P. De Marco, F. Cirillo, A.R. Cappello, V. Dolce, A. Belfiore, M. Maggiolini, E.M. De Francesco, Copper activates HIF-1alpha/GPER/VEGF signalling in cancer cells, *Oncotarget* 6 (2015) 34158–34177, <https://doi.org/10.18632/oncotarget.5779>.
- [25] L. Pickart, J.M. Vasquez-Soltero, A. Margolina, The effect of the human peptide GHK on gene expression relevant to nervous system function and cognitive decline, *Brain Sci.* 7 (2017), <https://doi.org/10.3390/brainsci7020020>.
- [26] H. Li, P.Z. Toh, J.Y. Tan, M.T. Zin, C.Y. Lee, B. Li, M. Leolukman, H. Bao, L. Kang, Selected biomarkers revealed potential skin toxicity caused by certain copper compounds, *Sci. Rep.* 6 (2016) 37664, <https://doi.org/10.1038/srep37664>.
- [27] L. Pickart, J.M. Vasquez-Soltero, A. Margolina, The human tripeptide GHK-Cu in prevention of oxidative stress and degenerative conditions of aging: implications for cognitive health, *Oxidative Med. Cell. Longev.* 324832 (2012), <https://doi.org/10.1155/2012/324832>.
- [28] T.D. Luong, M. Zoughaib, R. Garifullin, S. Kuznetsova, M.O. Guler, T.I. Abdullin, In situ functionalization of poly(hydroxyethyl methacrylate) cryogels with oligopeptides via  $\beta$ -cyclodextrin–adamantane complexation for studying cell-instructive peptide environment, *ACS Appl. Bio Mater.* 3 (2020) 1116–1128, <https://doi.org/10.1021/acsabm.9b01059>.
- [29] T. Wen, F. Qu, N.B. Li, H.Q. Luo, A facile, sensitive, and rapid spectrophotometric method for copper(II) ion detection in aqueous media using polyethyleneimine, *Arab. J. Chem.* 10 (2017) S1680–S1685, <https://doi.org/10.1016/j.arabjc.2013.06.013>.

- [30] O.V. Tsepaeva, A.V. Nemtarev, T.I. Abdullin, L.R. Grigor'eva, E.V. Kuznetsova, R. A. Akhmadishina, L.E. Ziganshina, H.H. Cong, V.F. Mironov, Design, synthesis, and cancer cell growth inhibitory activity of triphenylphosphonium derivatives of the triterpenoid betulin, *J. Nat. Prod.* 80 (2017) 2232–2239, <https://doi.org/10.1021/acs.jnatprod.7b00105>.
- [31] M.H. Zoughaib, D.T. Luong, Z.Y. Siraeva, A.A. Yergeshov, T.I. Salikhova, S. V. Kuznetsova, R.G. Kiyamova, T.I. Abdullin, Tumor cell behavior in porous hydrogels: effect of application technique and doxorubicin treatment, *Bull. Exp. Biol. Med.* 167 (2019) 590–598, <https://doi.org/10.1007/s10517-019-04577-y>.
- [32] Z. Wang, Y. Zhang, J. Zhang, L. Huang, J. Liu, Y. Li, G. Zhang, S.C. Kundu, L. Wang, Exploring natural silk protein sericin for regenerative medicine: an injectable, photoluminescent, cell-adhesive 3D hydrogel, *Sci. Rep.* 4 (2014) 7064, <https://doi.org/10.1038/srep07064>.
- [33] A. Trapaidze, C. Hureau, W. Bal, M. Winterhalter, P. Faller, Thermodynamic study of Cu<sup>2+</sup> binding to the DAHK and GHK peptides by isothermal titration calorimetry (ITC) with the weaker competitor glycine, *J. Biol. Inorg. Chem.* 17 (2012) 37–47, <https://doi.org/10.1007/s00775-011-0824-5>.
- [34] L. Gu, J. Zhang, L. Li, Z. Du, Q. Cai, X. Yang, Hydroxyapatite nanowire composited gelatin cryogel with improved mechanical properties and cell migration for bone regeneration, *Biomed. Mater.* 14 (2019), 045001, <https://doi.org/10.1088/1748-605X/ab1583>.
- [35] D. Luong, A.A. Yergeshov, M. Zoughaib, F.R. Sadykova, B.I. Gareev, I.N. Savina, T. I. Abdullin, Transition metal-doped cryogels as bioactive materials for wound healing applications, *Mater. Sci. Eng. C* 103 (2019) 109759, <https://doi.org/10.1016/j.msec.2019.109759>.
- [36] H. Studenovska, P. Vodicka, V. Proks, J. Hlucilova, J. Motlik, F. Rypacek, Synthetic poly(amino acid) hydrogels with incorporated cell-adhesion peptides for tissue engineering, *J. Tissue Eng. Regen. Med.* 4 (2010) 454–463, <https://doi.org/10.1002/term.256>.
- [37] S. Jose, M.L. Hughbanks, B.Y. Binder, G.C. Ingavle, J.K. Leach, Enhanced trophic factor secretion by mesenchymal stem/stromal cells with glycine-histidine-lysine (GHK)-modified alginate hydrogels, *Acta Biomater.* 10 (2014) 1955–1964, <https://doi.org/10.1016/j.actbio.2014.01.020>.
- [38] D.J. Medina-Leyte, M. Domínguez-Pérez, I. Mercado, M.T. Villarreal-Molina, L. Jacobo-Albavera, Use of human umbilical vein endothelial cells (HUVEC) as a model to study cardiovascular disease: a review, *Appl. Sci.* 10 (2020) 938, <https://doi.org/10.3390/app10030938>.
- [39] H. Hu, Y. Tang, L. Pang, C. Lin, W. Huang, D. Wang, W. Jia, Angiogenesis and full-thickness wound healing efficiency of a copper-doped borate bioactive glass/poly (lactic-co-glycolic acid) dressing loaded with vitamin E in vivo and in vitro, *ACS Appl. Mater. Interfaces* 10 (2018) 22939–22950, <https://doi.org/10.1021/acsami.8b04903>.
- [40] A.H. Van Hove, K. Burke, E. Antonienko, E. Brown 3rd, D.S. Benoit, Enzymatically-responsive pro-angiogenic peptide-releasing poly(ethylene glycol) hydrogels promote vascularization in vivo, *J. Control. Release* 217 (2015) 191–201, <https://doi.org/10.1016/j.jconrel.2015.09.005>.
- [41] X. Wang, B. Liu, Q. Xu, H. Sun, M. Shi, D. Wang, M. Guo, J. Yu, C. Zhao, B. Feng, GHK-Cu-liposomes accelerate scald wound healing in mice by promoting cell proliferation and angiogenesis, *Wound Repair Regen.* 25 (2017) 270–278, <https://doi.org/10.1111/wrr.12520>.
- [42] C. Gaucher, A. Boudier, J. Bonetti, I. Clarot, P. Leroy, M. Parent, Glutathione: antioxidant properties dedicated to nanotechnologies, *Antioxidants (Basel)* 7 (2018), <https://doi.org/10.3390/antiox7050062>.
- [43] R.A. Akhmadishina, E.V. Kuznetsova, G.R. Sadrieva, L.R. Sabirzyanova, I. S. Nizamov, G.R. Akhmedova, I.D. Nizamov, T.I. Abdullin, Glutathione salts of O, O-diorganyl dithiophosphoric acids: synthesis and study as redox modulating and antiproliferative compounds, *Peptides.* 99 (2018) 179–188, <https://doi.org/10.1016/j.peptides.2017.10.002>.
- [44] H. Speisky, M. Gomez, F. Burgos-Bravo, C. Lopez-Alarcon, C. Jullian, C. Olea-Azar, M.E. Aliaga, Generation of superoxide radicals by copper-glutathione complexes: redox-consequences associated with their interaction with reduced glutathione, *Bioorg. Med. Chem.* 17 (2009) 1803–1810, <https://doi.org/10.1016/j.bmc.2009.01.069>.
- [45] I. Sóvágó, K. Várnagy, N. Lihi, Á. Grenács, Coordinating properties of peptides containing histidyl residues, *Coord. Chem. Rev.* 327–328 (2016) 43–54, <https://doi.org/10.1016/j.ccr.2016.04.015>.
- [46] J.H. Park, J. Yoon, B. Park, Pomolic acid suppresses HIF1 $\alpha$ /VEGF-mediated angiogenesis by targeting p38-MAPK and mTOR signaling cascades, *Phytomedicine.* 23 (2016) 1716–1726, <https://doi.org/10.1016/j.phymed.2016.10.010>.
- [47] J. Cheng, H.L. Yang, C.J. Gu, Y.K. Liu, J. Shao, R. Zhu, Y.Y. He, X.Y. Zhu, M.Q. Li, Melatonin restricts the viability and angiogenesis of vascular endothelial cells by suppressing HIF-1 $\alpha$ /ROS/VEGF, *Int. J. Mol. Med.* 43 (2019) 945–955, <https://doi.org/10.3892/ijmm.2018.4021>.
- [48] H. Cao, D. Yu, X. Yan, B. Wang, Z. Yu, Y. Song, L. Sheng, Hypoxia destroys the microstructure of microtubules and causes dysfunction of endothelial cells via the PI3K/Stathmin1 pathway, *Cell Biosci.* 9 (2019) 20, <https://doi.org/10.1186/s13578-019-0283-1>.
- [49] H.J. Sun, W.W. Cai, L.L. Gong, X. Wang, X.X. Zhu, M.Y. Wan, P.Y. Wang, L.Y. Qiu, FGF-2-mediated FGFR1 signaling in human microvascular endothelial cells is activated by vaccharin to promote angiogenesis, *Biomed. Pharmacother.* 95 (2017) 144–152, <https://doi.org/10.1016/j.biopha.2017.08.059>.
- [50] A. Li, M.L. Varney, J. Valasek, M. Godfrey, B.J. Dave, R.K. Singh, Autocrine role of interleukin-8 in induction of endothelial cell proliferation, survival, migration and MMP-2 production and angiogenesis, *Angiogenesis.* 8 (2005) 63–71, <https://doi.org/10.1007/s10456-005-5208-4>.
- [51] L.U. Ljungberg, M.M. Zegeye, C. Kardeby, K. Falker, D. Repsilber, A. Sirsjö, Global transcriptional profiling reveals novel autocrine functions of interleukin 6 in human vascular endothelial cells, *Mediat. Inflamm.* 2020 (2020) 4623107, <https://doi.org/10.1155/2020/4623107>.
- [52] L. Ju, Z. Zhou, B. Jiang, Y. Lou, X. Guo, Autocrine VEGF and IL-8 promote migration via Src/Vav2/Rac1/PAK1 signaling in human umbilical vein endothelial cells, *Cell. Physiol. Biochem.* 41 (2017) 1346–1359, <https://doi.org/10.1159/000465389>.
- [53] P.R. Sanberg, D.H. Park, N. Kuzmin-Nichols, E. Cruz, N.A. Hossne Jr., E. Buffolo, A. E. Willing, Monocyte transplantation for neural and cardiovascular ischemia repair, *J. Cell. Mol. Med.* 14 (2010) 553–563, <https://doi.org/10.1111/j.1582-4934.2009.00903.x>.
- [54] A. Endler, L. Chen, Q. Li, K. Uchida, T. Hashimoto, L. Lu, G.T. Xu, F. Shibasaki, Int6/eIF3e silenced HIF2 $\alpha$  stabilization enhances migration and tube formation of HUVECs via IL-6 and IL-8 signaling, *Cytokine.* 62 (2013) 115–122, <https://doi.org/10.1016/j.cyto.2013.01.021>.
- [55] M. Amoorahim, E. Valipour, Z. Hoseinkhani, A. Mahnam, D. Rezazadeh, M. Ansari, M. Shahlaei, Y.H. Gamizgy, S. Moradi, K. Mansouri, TSGA10 overexpression inhibits angiogenesis of HUVECs: a HIF-2 $\alpha$  biased perspective, *Microvasc. Res.* 128 (2020) 103952, <https://doi.org/10.1016/j.mvr.2019.103952>.
- [56] C.K. Domigan, C.M. Warren, V. Antanesian, K. Happel, S. Ziyad, S. Lee, A. Krall, L. Duan, A.X. Torres-Collado, L.W. Castellani, D. Elashoff, H.R. Christofk, A.M. van der Bliek, M. Potente, M.L. Iruela-Arispe, Autocrine VEGF maintains endothelial survival through regulation of metabolism and autophagy, *J. Cell Sci.* 128 (2015) 2236–2248, <https://doi.org/10.1242/jcs.163774>.
- [57] M.E. Klontzas, S. Reakasame, R. Silva, J.C.F. Morais, S. Vernardis, R.J. MacFarlane, M. Heliotis, E. Tsiridis, N. Panoskaltis, A.R. Boccaccini, A. Mantalaris, Oxidized alginate hydrogels with the GHK peptide enhance cord blood mesenchymal stem cell osteogenesis: a paradigm for metabolomics-based evaluation of biomaterial design, *Acta Biomater.* 88 (2019) 224–240, <https://doi.org/10.1016/j.actbio.2019.02.017>.
- [58] L. Mazurowska, M. Mojski, ESI-MS study of the mechanism of glycyl-l-histidyl-l-lysine-Cu(II) complex transport through model membrane of stratum corneum, *Talanta.* 72 (2007) 650–654, <https://doi.org/10.1016/j.talanta.2006.11.034>.
- [59] J.J. Hostynek, F. Dreher, H.I. Maibach, Human skin penetration of a copper tripeptide in vitro as a function of skin layer, *Inflamm. Res.* 60 (2011) 79–86, <https://doi.org/10.1007/s00011-010-0238-9>.